GEOPHYSICAL RESEARCH LETTERS, VOL. 36, L01703, doi:10.1029/2008GL036203, 2009

Transient response of severe thunderstorm forcing to elevated greenhouse gas concentrations

Robert J. Trapp,[1] Noah S. Diffenbaugh,[1] and Alexander Gluhovsky[1]

Received 2 October 2008; accepted 20 November 2008; published 3 January 2009.

[1] We investigate the transient response of severe-thunderstorm forcing to the time-varying greenhouse gas concentrations associated with the A1B emissions scenario. Using a five-member ensemble of global climate model experiments, we find a positive trend in such forcing within the United States, over the period 1950–2099. The rate of increase varies by geographic region, depending on (i) low-level water vapor availability and transport, and (ii) the frequency of synoptic-scale cyclones during the warm season. Our results indicate that deceleration of the greenhouse gas emissions trajectory would likely result in slower increases in severe thunderstorm forcing. **Citation:** Trapp, R. J., N. S. Diffenbaugh, and A. Gluhovsky (2009), Transient response of severe thunderstorm forcing to elevated greenhouse gas concentrations, *Geophys. Res. Lett.*, *36*, L01703, doi:10.1029/2008GL036203.

1. Introduction

[2] Deep convective storms are ubiquitous worldwide. They represent a critical component in the hydrological cycle, and also play essential roles in large-scale atmospheric circulations by vertically mixing heat, water vapor, and momentum over the depth of the troposphere.

[3] But thunderstorms and their byproducts are also a natural hazard, as highlighted by the 1296 tornadoes that have occurred in the United States during the first six months of 2008 [*NOAA*, 2008]. This cumulative tornado count exceeds the average number of tornadoes for the entire year. Numerous instances of flash floods, lightning, hail, and destructive surface winds have also been reported, and underscore the significant threat to life and property that the extreme or severe modes of thunderstorms pose.

[4] The extent to which anomalous years such as 2008 are a consequence of internal climate system variability or of changes in external forcing of the climate system is currently unknown. Possible sources of internal variability include the El Niño-Southern Oscillation, although correlations between sea surface temperatures in the Pacific Ocean and tornado activity in the United States have been shown to be weak [*Marzban and Schaefer*, 2001]. Possible external changes include enhanced radiative forcing associated with human-induced increases in greenhouse gas (GHG) concentrations. Although the chaotic nature of the climate system renders attempts to attribute individual episodes of severe weather to anthropogenic effects tenuous at best, we can explore the links between *local phenomena* such as severe, extratropical thunderstorms to *global-scale* radiative processes. This is the motivation for our research.

[5] Herein we consider the transient response of severe, extratropical thunderstorm forcing to time-increasing GHG concentrations, thereby pursuing scale connections driven by the long-term impact of anthropogenically enhanced radiative processes. As demonstrated below, a key link in this connection is low-level atmospheric water vapor. An increase in water vapor is a consistent response to low-level warming [e.g., *Held and Soden*, 2006], and both can lead to enhanced buoyant energy for thunderstorm updrafts. Temperature itself is another key link: A reduction in the latitudinal temperature gradient implies a reduction in the vertical gradient of wind, which in turn implies the possibility of reduced thunderstorm organization and severity. Intermediary to these links are regional-scale, extratropical cyclones and attendant weather systems. The cyclones are in part governed by—but also help regulate—the temperature and humidity distributions. Hence, we turn to climate model experiments to help us identify the dominant processes and explore more deeply their implications for convective storm forcing.

2. Methods

[6] In order to quantify the transient response of severe thunderstorm forcing to transient changes in anthropogenic GHGs, we generated a five-member ensemble of experiments using the National Center for Atmospheric Research (NCAR) Community Climate System Model (CCSM3) [*Collins et al.*, 2006]. Given the CCSM3 c, e, b.ES01, f.ES01, and g.ES01 ensemble members produced by NCAR as part of the IPCC AR4 effort [*Meehl et al.*, 2007], we re-ran the atmospheric component of CCSM3 (CAM3), applying the original CCSM3-generated SSTs as a prescribed boundary condition, along with the same land cover and topography (following *Diffenbaugh et al.* [2006]). These new simulations provided the sub-daily, 3D atmospheric fields necessary for the thunderstorm forcing analyses.

[7] We integrated the five CAM3 ensemble members over the period 1948–2099, applying the greenhouse gas concentrations from the A1B emissions scenario (in which the total CO_2 concentrations increase to almost 700 ppm by end of the 21st century [*Nakićenović et al.*, 2000]), and allowing the initial three years for model spin-up. Each of the CAM3 simulations has 26 hybrid levels in the vertical and uses 85-wavenumber triangular truncation (T85) in the horizontal. Although this horizontal resolution is high for the current generation of GCMs [*Intergovernmental Panel on Climate Change*, 2007], it is obviously insufficient to represent individual thunderstorms. We can, however, exploit the resolved distributions of temperature, moisture, and

[1]Department of Earth and Atmospheric Sciences and Purdue Climate Change Research Center, Purdue University, West Lafayette, Indiana, USA.

0094-8276/09/2008GL036203$05.00

winds, which are well known to strongly influence the organization of cumulus clouds into severe convective storms [e.g., *Klemp*, 1987]. Validation of CCSM3 against global reanalysis data provides further justification for this general approach [*Marsh et al.*, 2007].

[8] We quantified severe thunderstorm forcing through an empirical parameter N_{DSEV} [*Brooks et al.*, 2003; *Trapp et al.*, 2007a; *Marsh et al.*, 2007], which represents the number of days on which significant surface winds, hail, and/or tornadoes could occur locally (in the vicinity of a model grid point), contingent on initiation of thunderstorms. This parameter was incremented on each model day (t), at each horizontal model grid point (x, y), as follows:

$$N_{DSEV}(x,y,t) = 1, CAPE \times S06 \geq 10000, \quad (1a)$$

$$N_{DSEV}(x,y,t) = 0, CAPE \times S06 < 10000 \quad (1b)$$

where the deep-layer wind shear S06 is given as the magnitude of the vector difference between the horizontal wind at 6 km AGL ($\vec{V}_6$) and the wind at the lowest model level ($\vec{V}_0$), and CAPE is convective available potential energy. Prior to the application of equation (1), we required that: CAPE $\geq$ 100 J kg^{-1}, $|\vec{V}_6| \geq |\vec{V}_0|$, $\geq$ 5m s^{-1}, and S06 $\geq$ 5 m s^{-1}.

[9] An acknowledged limitation to the methodology based on equation (1) is that it does not account for thunderstorm initiation. We have attempted to at least partially address this limitation through a new parameter $N_{DSEV,P}$. This is a measure of severe thunderstorm forcing constrained by the local occurrence of convective precipitation, and therefore by the local activation of model-parameterized cumulus convection [see *Collins et al.*, 2006]. Hence, $N_{DSEV,P}$ was incremented on each model day, at each horizontal model grid point, when equation (1a) was satisfied and the convective precipitation was nonzero.

[10] Time series of the forcing and other parameters were constructed for each ensemble member from spatial averages (denoted by $\langle\ \rangle$) over the following U.S. regions: southeast (SE; 75–95°W, 25–37.5°N), northeast (NE; 67.5–80°W, 37.5–47.5°N), Midwest (MW; 80–95°W, 37.5–50°N), southern Great Plains (SGP; 95–105°W, 25–40°N), and northern Great Plains (NGP; 95–105°W, 40–50°N). These regions were identified based on our previous research [*Trapp et al.*, 2007a], and considered particularly relevant for the current problem.

[11] Estimation of trends with simultaneous confidence bands was carried out following *Wu and Zhao* [2007] for data observed from the model

$$X_t = \mu_t + e_t, \quad t = 1, \ldots, n, \quad (2)$$

where μ_t is the unknown trend (a regression function) and e_t is a mean 0 stationary process. Assuming the trend is smooth (with subsequent testing of the residuals), it was computed via local polynomial regression [*Fan and Yao*, 2003] with the data-based global bandwidth selection [*Ruppert et al.*, 1995] and a bias correction. In future work, more complex trends will be treated with local polynomial regression with a local (dependent on t) bandwidth selection [*Ruppert*, 1997; *Gluhovsky and Gluhovsky*, 2007] or wavelet-based trend assessment.

[12] The construction of confidence bands with asymptotically correct coverage probabilities in case of dependent errors e_t is a major recent advancement attained by reducing equation (2) to the conventional model

$$\tilde{X}_t = \mu_t + \sigma Z_t, \quad t = 1, \ldots, n, \quad (3)$$

where Z_t are independent standard normal variables and σ^2 is the (unknown) variance of e_t. While with properly chosen bandwidths, the asymptotic properties of X_t follow those of $\tilde{X}_t$, it has become clear that even slight departures from normality may be detrimental for the inference based on finite samples [*Wilcox*, 2003] and time series records of limited length [*Gluhovsky and Agee*, 2007], which could be remedied by employing increasingly popular bootstrap methods. These were used in this paper for obtaining reliable inference for correlations, but bootstrap methods for estimating trends are still under development.

[13] Finally, we adopted the methodology of *Finnis et al.* [2007] and employed an objective means to identify cyclones in the CCSM3-simulated sea-level pressure fields. Monthly cyclone counts were then stratified by U.S. region and season. We then considered the cyclone counts during 20th and 21st Century time slices of 1980–1999 and 2080–2099, respectively. We computed the difference between the two sample means $\bar{x}$, normalized by the standard error for the difference:

$$z = \frac{\bar{x}_{21C} - \bar{x}_{20C}}{\sqrt{\frac{s^2_{21C}}{n} + \frac{s^2_{20C}}{n}}}, \quad (4)$$

where s^2 is the sample variance, and $n = 20 \times 12$ months. Absolute values of the test statistic z greater than 1.645 represent statistically significant differences at the 90% confidence level.

3. Results

[14] We begin with an analysis of thunderstorm intensity, a characterization that actually is rather ill defined. Although there is no accepted thunderstorm intensity metric, the updraft or vertical-wind speed within the storm is most often used and hence adopted herein. Strong thunderstorm updrafts are more likely to support the growth of large hailstones and produce large rainfall rates, which can lead to more intense downdrafts and associated outflow winds. Strong updrafts also tend to have large vertical gradients in vertical wind speed, which can stretch and amplify storm-scale rotation. Upon making a number of assumptions, it can be shown that $w_{max} = \sqrt{2 \times CAPE}$, where w_{max} is the theoretical maximum updraft speed [*Holton*, 2004]. Hence CAPE can serve as an indirect proxy for intensity.

[15] Observational data show that CAPE > 2000 J kg^{-1} occurs relatively infrequently (only a few days per year in the United States), though more often in the Great Plains [*Brooks et al.*, 2003]. One could conclude by way of this proxy that thunderstorms with high-end intensity are most frequent in geographical locations where the days with CAPE > 2000 J kg^{-1} ($CAPE_{2000}$) is largest. Our CCSM3

time series of regionally averaged $CAPE_{2000}$ allow us to draw further conclusions about long-term future trends in high-end thunderstorms. Over the interval 1950–2099, slight increases in $\langle CAPE_{2000} \rangle$ are indicated over the SE, MW, and NE regions (Figure 1a). On the other hand, fairly steep increases are indicated in the SGP and NGP regions. Thus, our climate model analysis suggests an increasing frequency of thunderstorms with strong updrafts over the Great Plains of the United States, a geographical region currently prone to such intense storms.

[16] An association between increases in convective storm updraft speeds and enhanced atmospheric GHGs has also been identified through a different means [*Del Genio et al.*, 2007]. Yet, an analysis of severe convective storm forcing is incomplete without consideration of the vertical shear of the environmental horizontal wind over the lower half of the troposphere (S06). Indeed, deep cumulus convection in the presence of large wind shear is modified such that subsequent organization, intensity, and longevity are enhanced given sufficient CAPE [*Weisman and Klemp*, 1982]. Hence, it is appropriate to combine both parameters into an empirical variable such as N_{DSEV}.

[17] It has been demonstrated that N_{DSEV} may undergo significant increases by the late 21st Century [*Trapp et al.*, 2007a]. Analysis of the temporal pathway to such elevated thunderstorm forcing is now possible with our continuous model integrations. Over each of the five regions considered, a positive trend in $\langle N_{DSEV} \rangle$ is revealed in the time series of a representative ensemble member as well as in the ensemble mean (Figure 1b). Importantly, the long-term trend in this variable is also smooth rather than abrupt. A weaker, yet still statistically significant positive trend in the forcing constrained by occurrence of convective-precipitation $\langle N_{DSEV,P} \rangle$ is also indicated for each of the regions (Figure 1c). In the least, this suggests that the frequency of thunderstorm initiation, or conversely of thunderstorm inhibition, does not appear to undergo substantial change in response to elevated greenhouse gas concentrations (see below).

[18] The severe-thunderstorm forcing increases in time in spite of the decreases in vertical wind shear (Figure 1d), and because of compensating increases in CAPE (Figure 1e). Potential contributors to CAPE include the temperature lapse rate in the middle troposphere, the boundary-layer temperature, and the boundary-layer water vapor [e.g., *Brooks et al.*, 2003]. For the current experiments, these are listed in increasing order of importance, with essentially no long-term trend indicated in the temperature lapse rates over a 3–5 km AGL layer (not shown), and a statistically significant positive trend in specific humidity q (Figure 1f). Considerable linear correlation between changes in CAPE and changes in q (Table 1) reinforces this attribution. Such low-level humidification in these extratropical regions owes in part to in-situ evaporation, but also to remote evaporation and subsequent transport (we note that atmospheric transport in this and other GCMs can be sensitive to the numerical formulation [e.g., *Stenke et al.*, 2008; *Rasch et al.*, 2006]). In other words, the effects of anthropogenically enhanced GHGs on convection are considerably nonlocal [*Trenberth*, 1999].

[19] Indeed, much of the extratropical water-vapor (and also heat) originates in the subtropics and is transported poleward by synoptic-scale cyclones [*Trenberth*, 1999]. The thermodynamic and dynamic processes associated with extratropical cyclones otherwise pre-condition the atmosphere for deep convective clouds and subsequently help initiate their formation. The release of latent heat due to the clouds has an upscale effect that can then intensify cyclones. Therefore, our projected increases in severe thunderstorm forcing would at first glance appear to be at odds with previous analyses projecting future decreases in cyclone frequency [e.g., *Finnis et al.*, 2007].

[20] Over the conterminous United States, our analysis clearly shows a decrease in annual cyclone frequency during the model integration period (Figure 2). However, closer inspection of the monthly and seasonal counts shows that most of this decrease occurs during winter and early spring months. Statistically significant decreases in the 21st Century cyclone frequency are found in most ensemble members during the months relatively less prone to midlatitude thunderstorm formation (NDJF, or "cool season"). In contrast, statistically insignificant decreases and even increases in cyclone frequency are generally found in the ensemble members during the late spring and summer months (AMJJ, or "warm season"), which tend to be relatively more prone to thunderstorm formation (Figure 2). Although occurrence of a severe thunderstorm is not exclusively linked to existence of a synoptic-scale cyclone, we do note for example that in the SE (NGP) region, the little change (decreases) in the warm-season cyclone frequency corresponds well with the large (weak) trends in $\langle N_{DSEV} \rangle$. Hence, from the perspective of a time-varying regional analysis, we can conclude that projected changes in severe thunderstorm forcing are actually quite congruous with projected changes (or lack thereof) in synoptic-scale cyclone frequency.

[21] A synthesis of our results and theory now provides us with a relatively simple yet compelling way to connect anthropogenically enhanced global-scale processes to changes in hazardous convective-scale phenomena. A key link is low-level atmospheric water vapor. Low-level warming from radiative processes results in in-situ low-level humidification [e.g., *Held and Soden*, 2006], given some supply of moisture from a water body and/or vegetation. Humidification also results from remote evaporation and subsequent transport, which depends in part on extratropical cyclones and their associated winds. Enhanced low-level water vapor (and low-level warming) then adds to existing local static instability of the atmosphere. A final consequence is locally enhanced buoyant energy (or CAPE), which can be realized as enhanced thunderstorm updrafts.

[22] The physical interactions do not terminate at this scale, since latent heating can then intensify the synoptic-scale cyclones, and thereby feed back into vapor transport and thunderstorm initiation. Countering this diabatic effect on cyclone intensification, however, is the reduction of large-scale, low-level baroclinity, resulting from the latitudinally varying radiative forcing, including surface albedo feedbacks [e.g., *Holland and Bitz*, 2003; *Geng and Sugi*, 2003; *Finnis et al.*, 2007]. Hence, the low-level temperature itself constitutes another key link, albeit one that varies by season and by geographical region. Indeed, the reduction in baroclinity is associated with a reduction in vertical wind shear, as mandated by the thermal wind equation. This implies a locally reduced contribution to severe thunderstorm

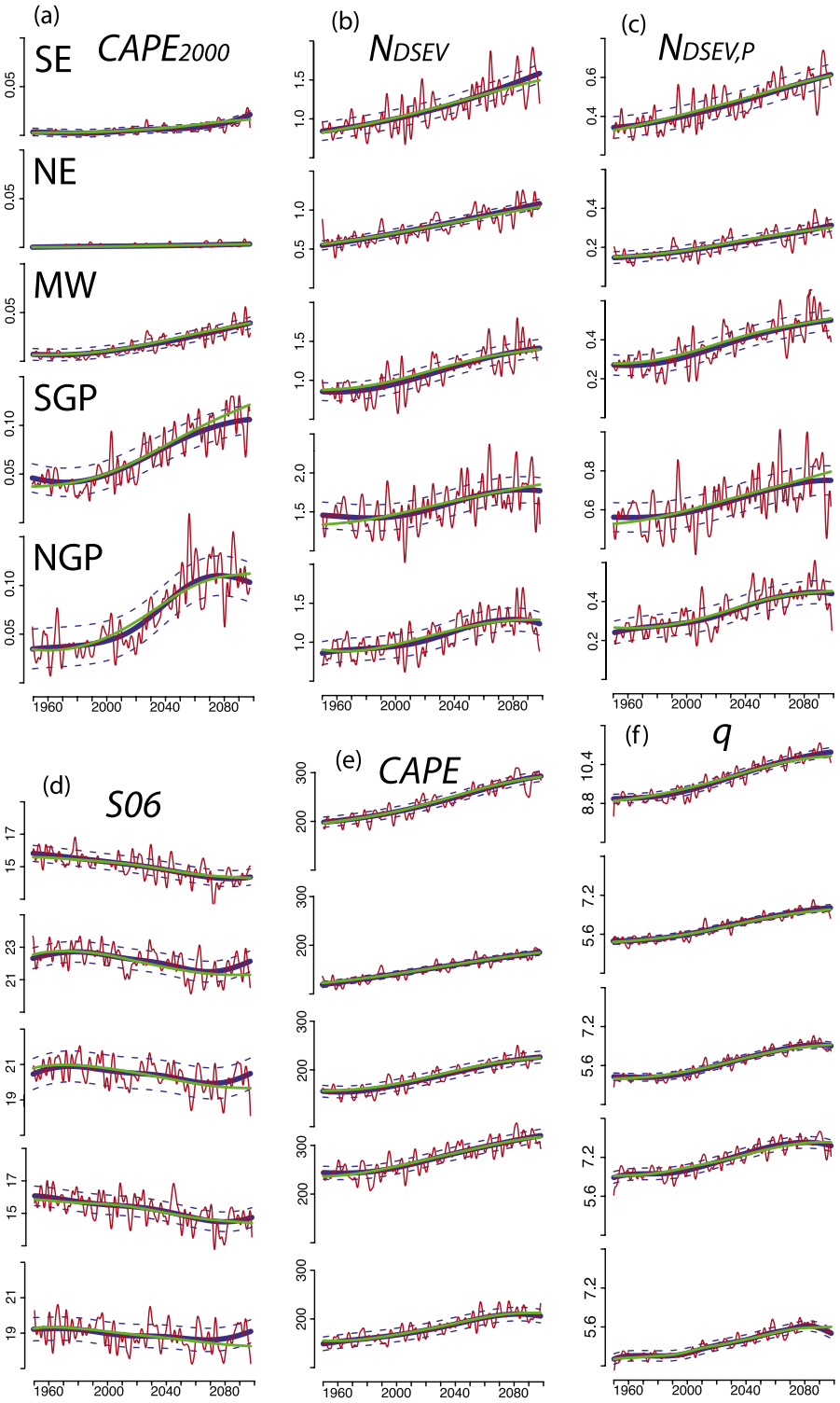

Figure 1. Time series of regionally averaged: (a) $CAPE_{2000}$, the number of days on which CAPE > 2000 J kg^{-1}, (b) N_{DSEV}, the number of days on which severe convective storms and associated significant surface winds, hail, and/or tornadoes could occur in the vicinity of a grid point, (c) $N_{DSEV,P}$, the number of days with the joint occurrence of severe convective storm forcing and convective precipitation at a grid point, (d) S06, the magnitude of the vector difference between the horizontal wind at 6 km AGL and the wind at the lowest model level (m s^{-1}), (e) CAPE (J kg^{-1}), and (f) q, the surface specific humidity ($\times 10^{-3}$ kg kg^{-1}), for the SE, NE, MW, SGP, and NGP regions of the United States (see text). The bold blue line represents the trend, and the dashed blue lines give the 90% confidence bands. The red line is a local polynomial fit to the data, using a 12-month bandwidth. These time-series data originated from the ensemble member "b". The bold green line indicates the ensemble mean time series, analyzed using the same global bandwidth as that applied to the individual member. Note that since the time-series values are regional averages, and the time series are also filtered, the values are considerably less than what would be expected from raw data in smaller sub-areas within the regions.

Table 1. Linear Correlations Between Changes in CAPE and Changes in Surface Specific Humidity (q)[a]

Region	Member-b	Member-c	Member-e	Member-f	Member-g
SE	0.62 (.49, .72)	0.53 (.43, .62)	0.35 (.19, .50)	0.80 (.66, .80)	0.78 (.72, .84)
NE	0.70 (.59, .79)	0.51 (.34, .65)	0.05 (−.13, .24)	0.79 (.70, .87)	0.81 (.70, .91)
MW	0.90 (.86, .93)	0.81 (.76, .86)	0.34 (.21, .46)	0.73 (.73, .85)	0.89 (.85, .92)
SGP	0.77 (.68, .85)	0.37 (.10, .66)	0.51 (.29, .69)	0.69 (.53, .81)	0.49 (.26, .70)
NGP	0.50 (.27, .68)	0.55 (.39, .71)	0.38 (.09, .61)	0.60 (.40, .75)	0.80 (.71, .87)

[a]Changes are based on mean 21C (2079–2098) minus mean 20C (1979–1998) values. The 90% bootstrap confidence intervals are given in parentheses.

forcing from wind shear [see *Trapp et al.*, 2007a], the potential for less storm organization, and a potential decrease in severe thunderstorm forcing as GHG concentrations increase. However, our modeling results show that the net severe thunderstorm forcing continues to increase through the late 21st Century even with time-decreasing shear. This persistent increasing trend in N_{DSEV} is caused by the persistent increasing trend in CAPE, which is sufficient to overcome the decreases in shear.

4. Summary and Conclusions

[23] Our study shows that the frequency of severe-thunderstorm forcing increases in time in response to the

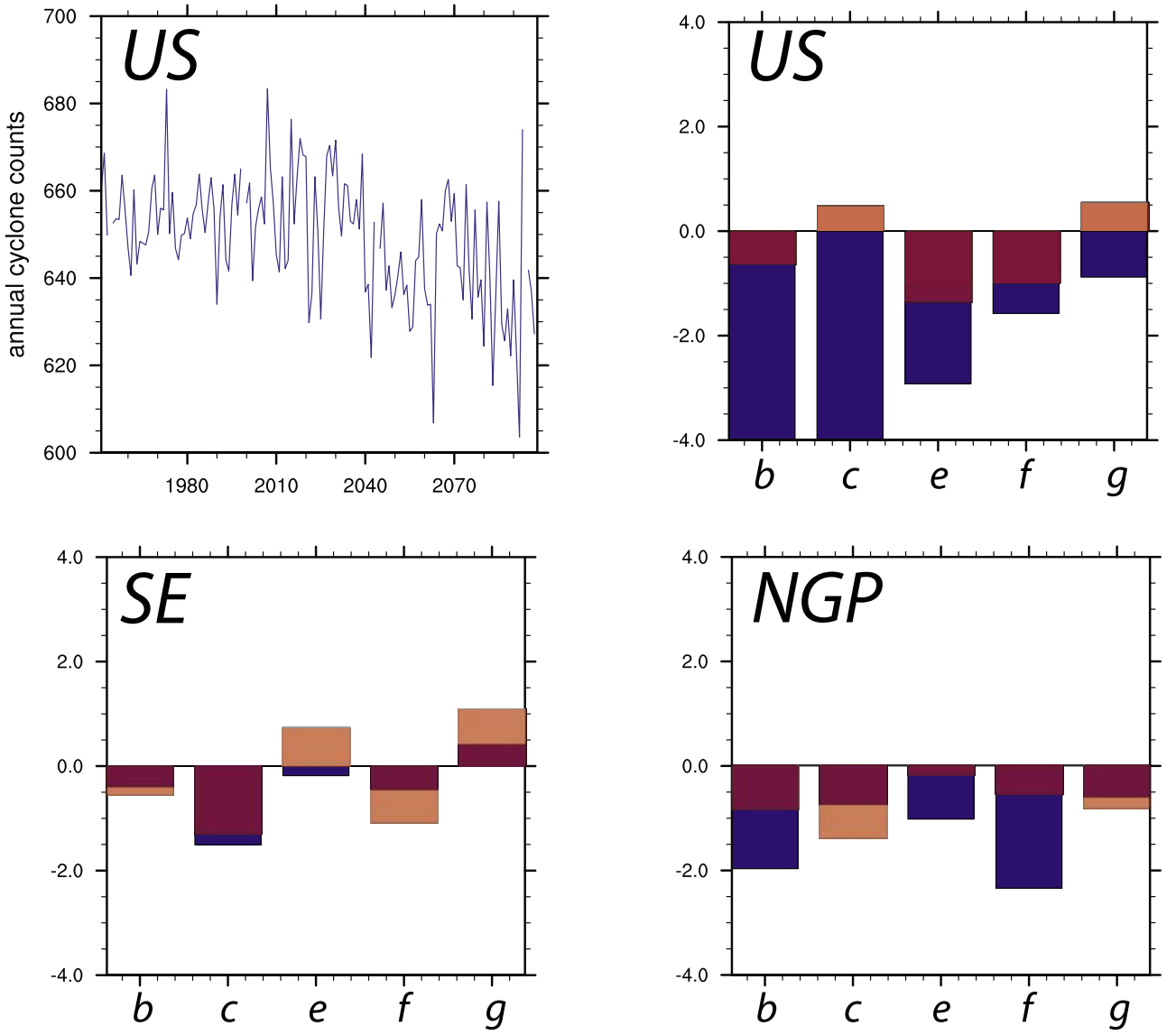

Figure 2. Ensemble mean time series of annual cyclone frequency over the conterminous United States, and differences, for each ensemble member (b, c, e, f, g) between the mean 21C (2080–2099) and 20C (1980–1999) cyclone frequency normalized by the standard error for the difference, during the AMJJ (red) and NDJF (blue) seasons: conterminous United States, and the SE and NGP regions.

A1B scenario of GHG emissions. This is also true for severe-thunderstorm forcing that is constrained by the occurrence of convective precipitation. The rate of increase varies with geographical region and inherently depends on (i) low-level water vapor availability and transport, and (ii) the frequency of midlatitude synoptic-scale cyclones during the warm season. The current report provides further evidence of the effect of anthropogenic GHG emissions on long-term trends in thunderstorm forcing [*Trapp et al.*, 2007a; *Del Genio et al.*, 2007]. Further, it is suggested that deceleration of the trajectory of GHG emissions could help reduce increases in severe convective weather in the coming decades.

[24] A consideration of other meteorological factors, and other approaches [*Trapp et al.*, 2007b], will be necessary to refine these conclusions for specific hazardous phenomena such as tornadoes. Furthermore, resolution of questions raised about individual anomalous years in storm occurrence awaits advanced statistical and high-resolution dynamical modeling.

[25] **Acknowledgments.** The authors acknowledge the helpful comments made by the two reviewers. This work stems from the Climate and Extreme Weather initiatives within the Department of Atmospheric Sciences at Purdue University and the Purdue Climate Change Research Center, and was supported in part by NSF ATM-0541491. This is PCCRC paper 0830.

References

Brooks, H. E., J. W. Lee, and J. P. Craven (2003), The spatial distribution of severe thunderstorm and tornado environments from global reanalysis data, *Atmos. Res.*, *67–68*, 73–94.

Collins, W. D., et al. (2006), The Community Climate System Model Version 3 (CCSM3), *J. Clim.*, *19*, 2122–2143.

Del Genio, A. D., M.-S. Yao, and J. Jonas (2007), Will moist convection be stronger in a warmer climate?, *Geophys. Res. Lett.*, *34*, L16703, doi:10.1029/2007GL030525.

Diffenbaugh, N. S., M. Ashfaq, B. Shuman, J. W. Williams, and P. J. Bartlein (2006), Summer aridity in the United States: Response to mid-Holocene changes in insolation and sea surface temperature, *Geophys. Res. Lett.*, *33*, L22712, doi:10.1029/2006GL028012.

Fan, J., and Q. Yao (2003), *Nonlinear Time Series*, 551 pp., Springer, New York.

Finnis, J., M. M. Holland, M. C. Serreze, and J. J. Cassano (2007), Response of Northern Hemisphere extratropical cyclone activity and associated precipitation to climate change, as represented by the Community Climate System Model, *J. Geophys. Res.*, *112*, G04S42, doi:10.1029/2006JG000286.

Geng, Q., and M. Sugi (2003), Possible change of extratropical cyclone activity due to enhanced greenhouse gases and sulfate aerosols: Study with a high-resolution AGCM, *J. Clim.*, *16*, 2262–2274.

Gluhovsky, A., and E. M. Agee (2007), On the analysis of atmospheric and climatic time series, *J. Appl. Meteorol. Climatol.*, *46*, 1125–1129.

Gluhovsky, I., and A. Gluhovsky (2007), Smooth location dependent bandwidth selection for local polynomial regression, *J. Am. Stat. Assoc.*, *102*, 718–725.

Held, I. M., and B. J. Soden (2006), Robust responses of the hydrological cycle to global warming, *J. Clim.*, *19*, 5686–5699.

Holland, M. M., and C. M. Bitz (2003), Polar amplification of climate change in coupled models, *Clim. Dyn.*, *21*, 221–232.

Holton, J. R. (2004), *An Introduction to Dynamic Meteorology*, 535 pp., Academic, New York.

Intergovernmental Panel on Climate Change (2007), *Climate Change 2007: The Physical Science Basis. Contribution of Working Group I to the Fourth Assessment Report of the Intergovernmental Panel on Climate Change*, edited by S. Solomon et al., Cambridge Univ. Press, Cambridge, U. K.

Klemp, J. B. (1987), Dynamics of tornadic thunderstorms, *Annu. Rev. Fluid Mech.*, *19*, 369–402.

Marsh, P. T., et al. (2007), Assessment of the severe weather environment in North America simulated by a global climate model, *Atmos. Sci. Lett.*, *8*, 100–106.

Marzban, C., and J. T. Schaefer (2001), The correlation between U.S. tornadoes and Pacific sea surface temperatures, *Mon. Weather Rev.*, *129*, 884–895.

Meehl, G. A., et al. (2007), THE WCRP CMIP3 multimodel dataset: A new era in climate change research, *Bull. Am. Meteorol. Soc.*, *88*, 1383–1394.

Nakićenović, N., et al. (2000), *Special Report on Emissions Scenarios: A Special Report of Working Group III of the Intergovernmental Panel on Climate Change*, 599 pp., Cambridge Univ. Press, Cambridge, U. K.

NOAA (2008), Storm reports, http://www.spc.noaa.gov/climo, Natl. Clim. Data Cent., Asheville, N. C.

Rasch, P. J., et al. (2006), Characteristics of atmospheric transport using three numerical formulations for atmospheric dynamics in a single GCM, *J. Clim.*, *19*, 2243–2266.

Ruppert, D. (1997), Empirical-bias bandwidths for local polynomial nonparametric regression and density estimation, *J. Am. Stat. Assoc.*, *92*, 1049–1062.

Ruppert, D., S. J. Sheather, and M. P. Band (1995), An effective bandwidth selector for local least squares regression, *J. Am. Stat. Assoc.*, *90*, 1257–1270.

Stenke, A., V. Grewe, and M. Ponater (2008), Lagrangian transport of water vapor and cloud water in the ECHAM4 GCM and its impact on the cold bias, *Clim. Dyn.*, *31*, 491–506.

Trapp, R. J., et al. (2007a), Changes in severe thunderstorm environment frequency during the 21st century caused by anthropogenically enhanced global radiative forcing, *Proc. Natl. Acad. Sci. U. S. A.*, *104*, 19,719–19,723.

Trapp, R. J., B. A. Halvorson, and N. S. Diffenbaugh (2007b), Telescoping, multimodel approaches to evaluate extreme convective weather under future climates, *J. Geophys. Res.*, *112*, D20109, doi:10.1029/2006JD008345.

Trenberth, K. E. (1999), Conceptual framework for changes of extremes of the hydrological cycle with climate change, *Clim. Change*, *42*, 327–339.

Weisman, M. L., and J. B. Klemp (1982), The dependence of numerically simulated convective storms on vertical wind shear and buoyancy, *Mon. Weather Rev.*, *110*, 504–520.

Wilcox, R. R. (2003), *Applying Contemporary Statistical Techniques*, 608 pp., Academic, San Diego, Calif.

Wu, W. B., and Z. Zhao (2007), Inference of trends in time series, *J. R. Stat. Soc., Ser. B*, *69*, 391–410.

N. S. Diffenbaugh, A. Gluhovsky, and R. J. Trapp, Department of Earth and Atmospheric Sciences, Purdue University, 550 Stadium Mall Drive, West Lafayette, IN 47907, USA. (jtrapp@purdue.edu)